Role of Surfactant Type and Concentration for the Mean Drop Size during Emulsification in Turbulent Flow

Slavka Tcholakova,[†] Nikolai D. Denkov,*[,†] and Thomas Danner[‡]

Laboratory of Chemical Physics & Engineering, Faculty of Chemistry, Sofia University, 1 James Bourchier Avenue, 1164 Sofia, Bulgaria, and BASF Aktiengesellschaft, GCT/P, L549, Ludwigshafen, Germany

Received March 15, 2004. In Final Form: June 18, 2004

A systematic experimental study of the effect of several factors on the mean drop diameter, d_{32}, during emulsification, is performed with soybean oil-in-water emulsions. These factors are (1) type of used emulsifier; (2) emulsifier concentration, C_S; and (3) ionic strength of the aqueous solution. Three different types of emulsifier, anionic (sodium dodecyl sulfate, SDS), nonionic (polyoxyethylene-20 cetyl ether, Brij 58), and protein (whey protein concentrate), are studied. For all of the studied systems, two well-defined regions are observed in the dependence of d_{32} on C_S: at low surfactant concentration, d_{32} increases significantly with the decrease of C_S (region 1), whereas d_{32} does not depend on C_S at high surfactant concentration (region 2). The model, proposed by Tcholakova et al. (*Langmuir* **2003**, *19*, 5640), is found to describe well the dependence of d_{32} on C_S in region 1 for the nonionic surfactant and for the protein emulsifier at high electrolyte concentration, 150 mM NaCl. According to this model, a well defined minimal surfactant adsorption (close to that of the dense adsorption monolayer) is needed for obtaining an emulsion. On the other hand, this model is found inapplicable to emulsions stabilized by the ionic surfactant, SDS, and by the nonionic surfactant, Brij 58, at low electrolyte concentration. The performed theoretical analysis of drop−drop interactions, in the emulsification equipment, shows that a strong electrostatic repulsion between the colliding drops impedes the drop−drop coalescence in the latter systems, so that smaller emulsion drops are obtained in comparison with the theoretically predicted ones. The results for SDS-stabilized emulsions in region 1 are explained by a quantitative consideration of this electrostatic repulsion. The drop size in region 2 (surfactant-rich regime) is described very well by the Kolmogorov−Hinze theory of turbulent emulsification.

1. Introduction

The drop size distribution obtained in an emulsification process is a result of the competition between two opposite processes, drop breakage and drop−drop coalescence.[1−7] Both processes are promoted by the intensive stirring of the oil−water mixture inside the emulsification chamber. The outcome of emulsification depends mainly on four different types of factors: (1) hydrodynamic conditions in the mixing device, (2) viscosity ratio, (3) volume fraction of the oil and water phases, and (4) type and concentration of used emulsifier. The current study is focused on the dependence of the mean drop size during emulsification on the surfactant type, concentration, and adsorption and on electrolyte concentration.

A detailed discussion of the various factors affecting emulsification is presented by Walstra et al.[1,6,7] Theoretical analysis and experimental results showed that, in turbulent flow and excess of emulsifier (so-called "surfactant-rich regime"),[8] the mean drop diameter depends primarily on the power density of energy dissipation in the emulsification chamber, ϵ, and on the oil−water interfacial tension, σ_{OW}. In this regime, the mean drop size practically does not depend on surfactant concentration and is affected by the type of used surfactant mainly through the equilibrium value of σ_{OW}. The relative probability for drop−drop coalescence is rather low in this emulsification regime.

On the other hand, at lower emulsifier concentration, the mean drop size depends strongly on the emulsifier type and concentration.[2,8−20] It was shown experimentally[2,8−20] that the mean drop size rapidly decreases

* To whom correspondence should be addressed: Assoc. Prof. Nikolai Denkov. Phone: (+359-2) 962 5310. Fax: (+359-2) 962 5643. E-mail: nd@lcpe.uni-sofia.bg.

† Sofia University.

‡ BASF Aktiengesellschaft.

(1) Walstra, P. Formation of emulsions. *Encyclopedia of Emulsion Technology*; Marcel Dekker: New York, 1983; Chapter 2.

(2) Narsimhan, G.; Goel, P. Drop coalescence during emulsion formation in a high-pressure homogenizer for tetradecane-in-water emulsion stabilized by sodium dodecyl sulfate. *J. Colloid Interface Sci.* **2001**, *238*, 420.

(3) Nienow, A. W. Break-up, coalescence and catastrophic phase inversion in turbulent contactors. *Proceedings of the 3rd World Congress on Emulsions*, Lyon, France, 2002; Editeur: Paris, 2002.

(4) Liu, Sh.; Li, D. Drop coalescence in turbulent dispersions. *Chem. Eng. Sci.* **1999**, *54*, 5667.

(5) Coulaloglou, C. A.; Tavlarides, L. L Description of interaction processes in agitated liquid-liquid dispersions. *Chem. Eng. Sci.* **1977**, *32*, 1289.

(6) Walstra, P.; Smulders, P. E. A. Formation of emulsions. In *Proceedings of the 2nd World Congress on Emulsions*, Sept 1997, Bordeaux, France; Editeur: Paris, 1998; pp 68−74.

(7) Walstra, P.; Geurts, T. J.; Noomen, A.; Jellema, A.; van Boekel, M. A. J. S. *Dairy Technology*; Marcel Decker: New York, 1999.

(8) Taisne, L.; Walstra, P.; Cabane, B. Transfer of oil between emulsion droplets. *J. Colloid Interface Sci.* **1996**, *184*, 378.

(9) Mohan, S.; Narsimhan, G. Coalescence of protein-stabilized emulsions in a high-pressure homogenizer. *J. Colloid Interface Sci.* **1997**, *192*, 1.

(10) Das, K. P.; Kinsella, J. E. Droplet size and coalescence stability of whey protein stabilized milkfat peanut oil emulsions. *J. Food Sci.* **1993**, *58*, 439.

(11) Gopal, E. S. R. Principles of emulsion formation. In *Emulsion Science*; Sherman, P., Ed.; Academic Press: London, 1968.

(12) Euston, S. R.; Hirst, R. L.; Hill, J. P. The emulsifying properties of β-lactoglobulin genetic variants A, B and C. *Colloids Surf., B* **1999**, *12*, 193.

(13) Djakovic, L.; Dokic, P.; Radivojevic, P.; Sefer, I.; Sovilj, V. Action of emulsifiers during homogenization of o/w emulsions. *Colloid Polym. Sci.* **1987**, *265*, 993.

(14) van Aken, G. A.; Zoet, F. D. Coalescence in highly concentrated emulsions. *Langmuir* **2000**, *16*, 7131.

(15) Lobo, L.; Svereika, A. Coalescence during emulsification: 2. Role of small molecule surfactants. *J. Colloid Interface Sci.* **2003**, *261*, 498.

10.1021/la049335a CCC: $27.50
Published on Web 08/07/2004

with the increase of initial emulsifier concentration in this "surfactant-poor" regime. Significant differences were observed in this regime between the low-molecular-mass surfactants, on one side, and the proteins, on the other side, with respect to their properties as emulsifiers. In the case of oil-in-water (o/w) emulsions, stabilized by proteins (β-lactoglobulin, BLG, and whey protein concentrate, WPC), a well-defined emulsifier adsorption on the oil drop surface, Γ^*, was measured during the steady-state stage of emulsification experiments, performed under various conditions.[19,20] The experiments showed[20] that Γ^* could be considered as a characteristic of the protein emulsifier, which did not depend on the initial protein concentration, oil volume fraction, and hydrodynamic conditions during emulsification. This result means that the oil drops continued coalescing during emulsification, until a threshold value of the surfactant adsorption, Γ^*, was reached (see section 3.3.1 for further explanation). By comparing the value of Γ^* with the adsorption isotherms of the respective proteins, it was shown[19,20] that emulsions, stabilized by BLG or WPC, are obtained at a drop surface coverage $\theta^* = \Gamma^*/\Gamma_M \approx 0.95$ (defined as the ratio between the actual protein adsorption and the maximal adsorption in a protein monolayer), that is, when the adsorption monolayer is almost complete.

In contrast, Taisne et al.[8] obtained sodium dodecyl sulfate (SDS)-stabilized o/w emulsions at surfactant adsorption, Γ, which varied within 2 orders of magnitude, between 0.014 mg/m^2 and $\Gamma_M \approx 1.4$ mg/m^2, depending on the experimental conditions (i.e., θ varied between 0.01 and 1). Similar results were reported by Narsimhan and Goel.[2] The experimental data from these studies[2,8] showed that, in contrast to BLG- and WPC-stabilized emulsions, no characteristic threshold adsorption, Γ^*, could be defined for SDS-containing emulsions.

To clarify the reasons for the observed differences between low-molecular-mass surfactants and proteins, with respect to their emulsifying properties, we performed systematic experiments with soybean o/w emulsions in the presence of protein emulsifier, WPC (+150 mM NaCl), anionic surfactant SDS (+10 or 150 mM NaCl), and nonionic surfactant polyoxyethylene-20 cetyl ether (Brij 58; $+10^{-2}$ or 150 mM NaCl). These emulsions were prepared by means of a narrow-gap homogenizer under well-defined hydrodynamic conditions, and the relation between the mean drop size and emulsifier adsorption on one side and the type and initial concentration of emulsifier on the other side was studied. The experimental results are analyzed by considering the processes of drop breakup and drop−drop coalescence. Note that in this paper we analyze only the mean drop size during the steady-state stage of emulsification. The theoretical description of the kinetic aspects of the emulsification process (i.e., the rate of achieving this steady state) requires much more elaborated analysis of the interaction of the drops with the fluctuating pressure field of turbulent flow. Such an investigation is under way and will be described in a consecutive paper.

2. Materials and Methods

2.1. Materials. Two low-molecular-mass surfactants were used as received: anionic SDS (product of Acros) and nonionic Brij 58 (product of Sigma). As the protein emulsifier, we used WPC (trade name AMP 8000; product of Proliant). According to the certificate of AMP 8000, this protein concentrate of technical grade contains 71.7 wt % globular proteins (BLG as the main component), 17.2 wt % carbohydrates, 6.2 wt % water, 2.8 wt % ash, and 2.1 wt % fat. Commercial grade soybean oil was used as an oil phase, without additional purification. The aqueous solutions were prepared with deionized water, purified by a Milli-Q Organex system (Millipore). NaCl (product of Merck) was added to the surfactant solutions in concentrations of 0.01, 10, or 150 mM. The protein solutions contained also 0.01 wt % of the antibacterial agent NaN_3 (Riedel-de Haën).

2.2. Emulsion Preparation. Oil-in water emulsions were prepared by using a two-step procedure. Initially, an o/w premix was prepared by hand-shaking a vessel containing 200 mL of oil and 520 mL of an aqueous phase (28 vol % oil). The second homogenization step was accomplished by passing this premix, under pressure, through the slits of a narrow-gap homogenizer; see the scheme shown in Figure 1A. The width of the narrow slits in the homogenization chamber was 395 μm, and the driving pressure was 2.2×10^5 Pa. A closed loop (i.e., a circulation of the mixture) was used to ensure multiple passes of the oil−water mixture through the homogenizer and to achieve a steady-state drop size distribution.[20] The specimens for drop size analysis were taken by a pipet, from the outlet of the homogenizer, 10 min after starting the emulsification (this corresponded to 100 passes of the used 720 mL of the oil−water mixture). The temperature of the emulsion at the end of the emulsification experiments was 25 ± 1 °C. A more detailed description of the used emulsification procedure is presented in ref 20.

2.3. Determination of Drop Size Distribution. The drop size distribution was determined by optical microscopy. The specimens, taken from the outlet of the emulsification equipment, were immediately transferred in 1 wt % SDS solutions to (1) prevent further drop−drop coalescence and (2) reduce the drop concentration down to about 1 vol %, because the original emulsion was too concentrated for drop size analysis.

The SDS-stabilized specimens were transferred for optical examination into microcapillaries of rectangular cross sections (depth 0.1 mm, width 1 mm, length 40 mm) no longer than 1 h after their preparation. Before loading the sample into the microcapillary, the vial containing the SDS-stabilized emulsion was gently rotated at least 10 times to homogenize the emulsion. A series of measurements, performed after different periods of shelf storage of these SDS-stabilized specimens, proved that the drop size distribution remained unaltered for up to 2 days of storage. Therefore, the dispersion of the droplets in 1 wt % SDS solution efficiently conserved the drop size distribution from the emulsification outlet. As an additional check of the used procedure, for several of the studied samples, specimens for optical observation were prepared by diluting the original emulsion with 1 wt % solution of Brij 58. No difference in the measured drop size distributions was found between these two different dilution procedures.

The oil drops were observed in transmitted light with microscope Axioplan (Zeiss, Germany), equipped with objective Epiplan ×50, and connected to a charge-coupled device camera (Sony) and video recorder (Samsung SV-4000). During observation of a given region in the capillary, the focal plane of the microscope was gradually changed in depth of the emulsion to consecutively bring all drops into focus. The microscope focus and the light intensity were carefully controlled and optimized to obtain the sharpest possible boundaries between the oil drops and the surrounding aqueous medium. The size of a given drop was measured from the image, in which the drop exhibited the sharpest boundary. Note that no drop deformation (which could compromise the drop size determination) is expected in the studied systems, because the drop diameters were smaller than the depth of the used capillary (100 μm). The importance of drop

(16) Lobo, L. Coalescence during emulsification: 3. Effect of gelatin on rupture and coalescence. *J. Colloid Interface Sci.* **2002**, *254*, 165.

(17) Danner, T.; Schubert, H. Coalescence processes in emulsions. In *Food Colloids 2000, Fundamentals of Formulation*; Dickinson, E., Miller, R., Eds.; Royal Society of Chemistry: Cambridge, 2001; p 116.

(18) Danner, T.; Stang, M.; Schubert, H. Determination of droplet-coalescence in oil-in-water emulsions. In *Proceedings of the 3rd World Congress on Emulsions*, Lyon, France, 2002; Editeur: Paris, 2002.

(19) Tcholakova, S.; Denkov, N. D.; Ivanov, I. B.; Campbell, B. Coalescence in β-Lactoglobulin-Stabilized Emulsions: Effects of Protein Adsorption and Drop Size. *Langmuir* **2002**, *18*, 8960.

(20) Tcholakova, S.; Denkov, N. D.; Sidzhakova, D.; Ivanov, I. B.; Campbell, B. Interrelation between Drop Size and Protein Adsorption at Various Emulsification Conditions. *Langmuir* **2003**, *19*, 5640.

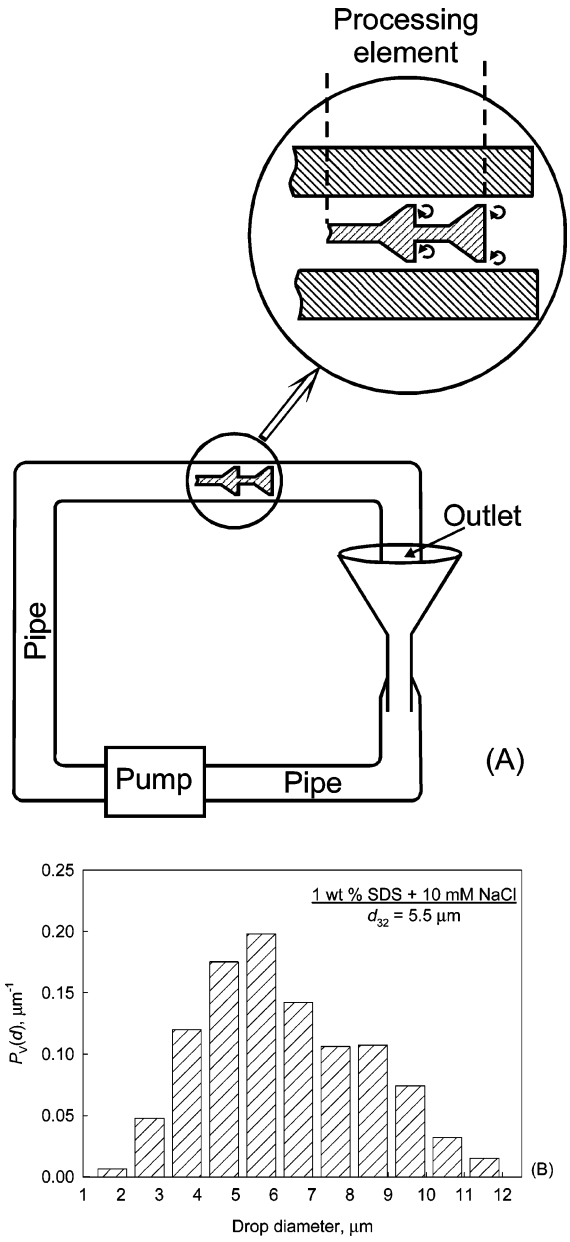

Figure 1. (A) Schematic presentation of the processing element and of the pipes in the used narrow-gap homogenizer. (B) Volume-weighted size distribution histogram of emulsion obtained with 1 wt % solution of SDS in the presence of 10 mM NaCl, at an oil volume fraction $\Phi = 0.28$. The gap width in the processing element was GW = 395 μm, and the pressure difference between the inlet and the outlet of the emulsification equipment was $\Delta P = 2.2 \times 10^5$ Pa.

deformation due to buoyancy could be evaluated by estimating the Bond number, $\Delta\rho g d^2/4\sigma_{OW}$, which represents the ratio of the gravity and capillary pressures ($\Delta\rho = 0.08$ g/cm^3 is the difference between the mass densities of the drop and continuous phases, g is acceleration of gravity, and σ_{OW} is interfacial tension). The estimates showed that the Bond number was always smaller than 10^{-4}, which indicated that the gravity-driven drop deformation was negligible.

The diameters of the recorded oil drops were measured one by one by an operator, using custom-made image analysis software working with a Targa+ graphic board (Truevision, U.S.A.). These data were numerically processed to obtain the drop size histogram. Note this procedure for image acquisition and analysis excludes the possibility of missing some of the drops, because the entire depth of the capillary containing the emulsion is scanned while changing the focus. The diameters of at least 5000 drops (from two to four independently prepared emulsions) were measured for each system.

An illustrative drop size histogram is shown in Figure 1B. The mean volume-surface diameter, d_{32}, was calculated from the relation

$$d_{32} = \frac{\sum N_i d_i^3}{\sum N_i d_i^2} \quad (1)$$

where N_i is the number of drops with diameter d_i.

2.4. Determination of Interfacial Tension. The interfacial tension of the studied solutions was measured by applying the drop-shape analysis to pendant oil drops.[21] The measurements were performed at 23.8 ± 0.2 °C.

3. Experimental Results and Discussion

3.1. Effect of Emulsifier Concentration on Mean Drop Size. In this subsection, we describe the main experimental results. Their explanation and discussion are presented in sections 3.2−3.4.

The effect of WPC concentration on drop size and protein adsorption, at various oil volume fractions, Φ, and hydrodynamic conditions during emulsification, was studied in ref 20. Hereafter, we reproduce only these results, which were obtained at a fixed oil volume fraction (Φ = 28%) and hydrodynamic conditions (gap width of the processing element in the homogenizer, GW = 395 μm), because the experiments for the present study were performed under these conditions with the other emulsifiers (SDS and Brij 58).

We found[20] with WPC solutions that the dependence of the mean volume-surface diameter, d_{32}, on the initial protein concentration, C_{PR}^{INI}, can be described by a curve consisting of two distinct regions (see Figure 2A): a significant decrease of d_{32} from about 30 μm down to 12 μm in the range of concentrations between 0.02 and 0.1 wt % (region 1) and a plateau region with $d_{32} \approx 7.5$ μm at concentrations above 0.2 wt % (region 2).

Qualitatively similar dependence was observed in the experiments, performed for the current study, with Brij 58 and SDS. The dependence of d_{32} on the initial concentration of Brij, C_S^{INI}, is plotted in Figure 2B, for both ionic strengths studied (10^{-2} and 150 mM). At the lower ionic strength (10^{-2} mM electrolyte), we observed that d_{32} decreased from 24 μm down to 6.2 μm in the range of Brij 58 concentrations between 8×10^{-3} and 0.1 wt % (region 1), followed by a plateau with $d_{32} \approx 6.2$ μm at concentrations above 0.1 wt % (region 2). A similar trend was observed at the higher electrolyte concentration (150 mM NaCl): d_{32} decreased from 40 μm down to 4.9 μm, followed by a plateau region at $C_S^{INI} > 0.1$ wt %. Note that, in the range of low surfactant concentrations, the mean drop size was significantly larger at 150 mM NaCl (as compared to the system containing electrolyte of lower concentration), whereas almost the same values of d_{32} were measured in the respective plateau regions.

The experiments with SDS solutions showed a similar dependence of d_{32} on C_S^{INI}, see Figure 2C. The drop size decreased from 12 μm down to 6 μm in the concentration range between 10^{-3} and 0.03 wt % SDS, followed by a plateau region with $d_{32} \approx 5.5$ μm at $C_S^{INI} > 0.1$ wt % (C_{NaCl} = 10 mM). In the presence of 150 mM NaCl, d_{32} decreased from 20 to 8.5 μm with the increase of C_S^{INI} from 10^{-3} up to 0.1 wt %. Similarly to Brij-containing emulsions, at higher NaCl concentration, the value of d_{32} is significantly

(21) Princen, H. M. The equilibrium shape of interfaces, drops, and bubbles. In *Surface and Colloid Science*; Matijevic, E., Ed.; Wiley: New York, 1969; Vol. 2; p 1.

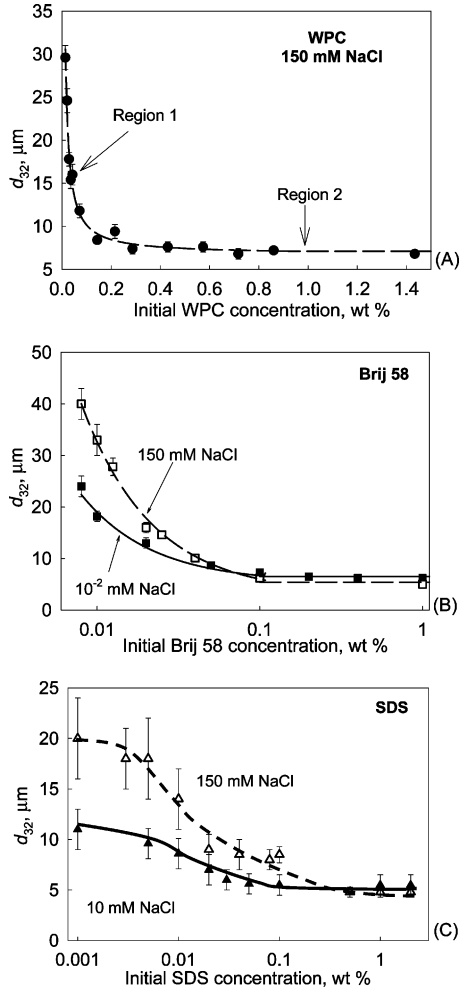

Figure 2. Mean volume-surface diameter, d_{32}, as a function of the initial emulsifier concentration, for emulsions stabilized by (A) WPC, (B) Brij 58, and (C) SDS, prepared at $\epsilon = 2.5 \times 10^8$ J/(m^3·s) and $\Phi = 0.28$.

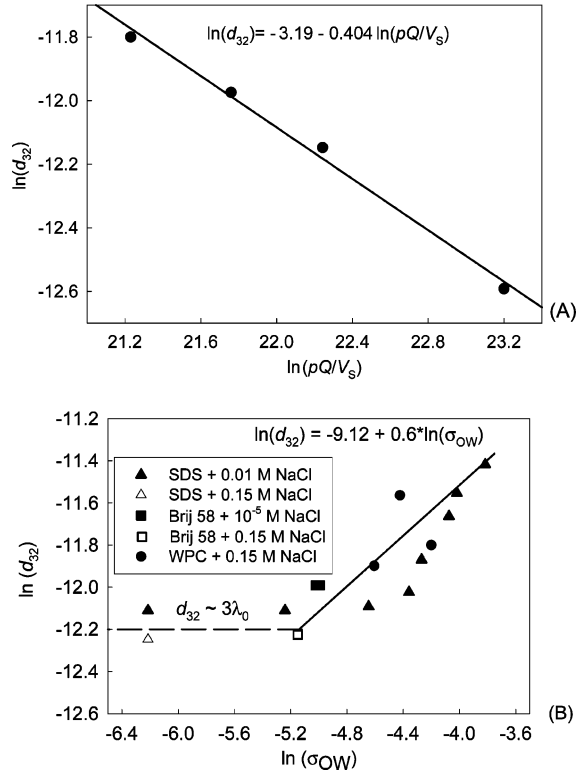

Figure 3. (A) Logarithm of the volume-surface diameter, d_{32}, versus the logarithm of pQ/V_S for emulsions stabilized by 3 wt % WPC at $\Phi = 0.28$, which were obtained with different narrow slits in the emulsification equipment.[20] The solid line represents the best fit used to estimate the dissipation volume, V_{DISS}; see section 3.2 for explanations. (B) Logarithm of d_{32} versus the logarithm of the interfacial tension, σ_{OW}, for emulsions prepared under equivalent hydrodynamic conditions, $\epsilon = 2.5 \times 10^8$ J/(m^3·s) and $\Phi = 0.28$. The symbols represent experimental data, whereas the continuous line represents the calculated values of d_{32} by eq 2; the horizontal dashed line corresponds to $d_{32} = 3\lambda_0$.

larger in the range of low surfactant concentrations ($C_{SDS} < 0.1$ wt %), whereas the values of d_{32} are almost the same in the plateau regions at both NaCl concentrations.

In conclusion, for all studied emulsifiers (protein, nonionic, and anionic surfactants; at high and low electrolyte concentrations) we observe two well-defined regions in the dependence of d_{32} on C_S^{INI}: a considerable decrease of drop size at low surfactant concentrations (region 1, $C_S^{INI} < 0.1$ wt %) and a plateau region at high surfactant concentrations (region 2, $C_S^{INI} > 0.1$ wt %).

3.2. Estimate of the Mean Drop Size in the Surfactant-rich Region 2. The fact that the mean drop size does not depend on emulsifier concentration in region 2 implies that the hydrodynamic conditions during emulsification play a decisive role at high emulsifier concentration.

The experimental data for d_{32}, measured in this region with WPC emulsions, were described in ref 20 by using the theory of turbulent emulsification.[1,7,22,23] According to this theory, the mean size of the drops, d_K, formed inside a developed isotropic turbulent flow, can be estimated by comparing the fluctuations of the hydrodynamic pressure in the flow with the capillary pressure of the drops. The respective equation for the mean drop diameter reads

$$d_K \sim \epsilon^{-2/5} \sigma_{OW}^{3/5} \rho_C^{-1/5} \quad (2)$$

where σ_{OW} is the interfacial tension, ρ_C is the mass density of the continuous phase, and ϵ is the average power density (rate of energy dissipation per unit volume) in the emulsification chamber. The power density can be found from the relation $\epsilon = \Delta P Q / V_{DISS}$, where ΔP is the pressure difference between the inlet and the outlet of the emulsification element, Q is the flow rate, and V_{DISS} is the volume of the mixing element, where the turbulent dissipation of energy takes place.

Equation 2 was used in ref 20 to estimate V_{DISS} by performing emulsification experiments at high WPC concentrations (in the protein-rich regime), with different processing elements, which had different gap widths and, thus, ensured different values of ΔP, Q, and ϵ. The mean volume-surface diameter, d_{32}, was measured by optical microscopy, and the plot of $\ln(d_{32})$ versus $\ln(\Delta PQ/V_S)$ was constructed under the assumption that $d_{32} \approx d_K$; see Figure 3A (V_S is the geometrical volume of the narrow slits in the homogenization chamber, which depends on the used processing element). As predicted by eq 2, the slope of the best linear fit, drawn through the experimental data, was found to be very close to −0.4 (see the straight line in

(22) Kolmogoroff, A. N. Drop breakage in turbulent flow. *Dokl. Akad. Nauk SSSR* **1949**, *66*, 825 (in Russian).
(23) Levich, V. G. *Physicochemical Hydrodynamics*; Prentice Hall: Englewood Cliffs, NJ, 1962.

Figure 3A). From the intercept of the line, taking into account that $\sigma_{OW} \approx 10$ mN/m and $\rho_C = 10^3$ kg/m^3, we estimated that the dissipation volume is $V_{DISS} \approx 10V_S$. The latter result shows that the actual turbulent zone extends in the space after the narrow slits as a result of the specific geometry of the used processing element. By using this estimate for V_{DISS}, we calculated[20] $\epsilon = 2.5 \times 10^8$ J/(m^3·s) for the processing element with gap width GW = 395 μm. This value of ϵ is used for theoretical estimates in the present study.

As one can see from eq 2, under fixed hydrodynamic conditions (given ϵ), d_{32} depends mainly on the interfacial tension, σ_{OW}. To check whether the theory of turbulent emulsification describes adequately the results, obtained with the other two emulsifiers, Brij 58 and SDS, we measured the equilibrium interfacial tension of the various solutions by means of the pendant drop method. The obtained results for ln(d_{32}) versus ln(σ_{OW}) are plotted in Figure 3B, versus the values of d_{32}, which are theoretically estimated by eq 2 (the continuous line). The comparison between the experimental data and the theoretical prediction shows that the agreement is satisfactory for $\sigma_{OW} > 5$ mN/m and $d_{32} > 5$ μm; see the continuous line in Figure 3B (no adjustable parameter is used for plotting this line).

On the other hand, we found that d_{32} remains constant ($d_{32} \approx 4.5$ μm, larger than the theoretical prediction, eq 2) at $\sigma_{OW} \leq 5$ mN/m; see the symbols around the horizontal dashed line in Figure 3B. To explain the latter experimental fact, we estimated the capillary number Ca $\approx 0.05 \ll 1$ (the respective equations can be found in section 3.3.4) and the viscosity ratio $\eta_D/\eta_C \approx 50$, for the viscous flow inside the smallest eddies, present in the turbulent flow during our experiments. The estimated small value of Ca and high value of η_D/η_C indicate that the viscous forces, inside the turbulent eddies, are not able to disrupt the oil drops in the studied systems (see, e.g., refs 1 and 6). Therefore, the drop size in our experiments should be limited from below by the size of the smallest eddies, λ_0. According to Kolmogorov's theory, λ_0 is given by the equation:[1,22,23]

$$\lambda_0 \sim \eta_C^{3/4} \rho_C^{-1/2} \epsilon^{-1/4} \tag{3}$$

where η_C is the dynamic viscosity of the continuous phase. Taking for our system $\eta_C \approx 1$ mPa·s, $\rho_C \approx 10^3$ kg/m^3, and $\epsilon \approx 2.5 \times 10^8$ J/(m^3·s), one can estimate that $\lambda_0 \approx 1.4$ μm, namely, the smallest average size, $d_{32} \approx 4.5$ μm, which we were able to obtain under the used hydrodynamic conditions, was approximately equal to $3\lambda_0$. For comparison, the measured minimal mean number diameter, $d_N \approx 2.5$ μm, was around $1.7\lambda_0$, and the left boundary of the drop size distribution curves (by number) corresponded approximately to λ_0. One can conclude from this analysis that the minimal drop size, observed in the experiments with various systems, was set by the size of the smallest turbulent eddies, λ_0.

Remarkably, we found that eq 2 describes reasonably well the data for d_{32} not only in the surfactant-rich region 2 for all studied emulsifiers but also in region 1 for the system SDS + 10 mM NaCl (see Figure 3B, where we have included all experimental points obtained with this system). This result means that the increased drop size in region 1 (as compared to the plateau region) could be entirely explained by the *variation of the interfacial tension* with the surfactant concentration for the system SDS + 10 mM NaCl. In other words, the data for this system can be explained without assuming the occurrence of drop−drop coalescence during emulsification in the entire concentration range of SDS that was studied (down to 10^{-3} wt %, which corresponds to 0.03 mM). Note that the initial SDS concentration in region 1 for this system was well below the critical micelle concentration of SDS, cmc ≈ 5 mM ≈ 0.15 wt % at 10 mM NaCl. For this system, SDS + 10 mM NaCl, the surfactant concentration in the aqueous phase during emulsification and the respective interfacial tension, σ_{OW}, were determined as explained in section 3.4 (eqs 23−25). For the other systems studied, the equilibrium interfacial tension, measured at the initial surfactant concentration C_S^{INI}, was used to plot Figure 3B, because the difference between C_S^{INI} and the concentration after emulsification, C_S^{SER}, was estimated to be negligible in region 2.

The attempts to describe the increased drop size in the surfactant-poor region 1, by means of eq 2 (i.e., by increase of σ_{OW} without drop−drop coalescence), were unsuccessful for all other systems studied by us (Brij 58, WPC, and SDS + 150 mM NaCl). As an example, if we assume that the drop−drop coalescence is insignificant during the emulsification process, we can estimate from eq 2 that the maximal mean drop diameter, according to Kolmogorov's theory, should be around 13 μm under the hydrodynamic conditions used,[24] whereas the experimental maximal values are considerably larger, between 20 and 40 μm. Therefore, we are certain that a significant re-coalescence occurred during emulsification in all emulsions with $d_{32} > 13$ μm; see Figure 2. That is why, in the following section 3.3, we consider the effect of drop−drop coalescence on d_{32}.

3.3. Estimate of Mean Drop Size in Region 1: Role of Drop−Drop Coalescence. *3.3.1. Phenomenological Model.* We start the analysis with a simple phenomenological model, originally proposed in ref 20, which was found to describe very well the data in region 1 for emulsions stabilized by WPC + 150 mM NaCl. The main assumption in the model is that the drops continue coalescing during emulsification until the surface protein adsorption reaches a certain threshold value, Γ^*. An additional assumption can be made to simplify the equations, namely, that virtually all emulsifier is adsorbed on the drop surfaces in the course of emulsification. These assumptions, applied to a mass balance of the used emulsifier (assumed equal to the adsorbed emulsifier), lead[20] to the following expression for d_{32}:

$$d_{32} \approx \frac{6\Phi}{1-\Phi} \frac{\Gamma^*}{C_S^{INI}} \tag{4}$$

where C_S^{INI} is the initial emulsifier concentration in the aqueous phase and Φ is the oil volume fraction. A more complex version of this phenomenological model was described in ref 20, in which the emulsifier adsorption isotherm, $\Gamma(C_S)$, was used to account for the emulsifier partitioning between the aqueous phase and the drop surface.[20] Instead of eq 4, a set of two algebraic equations was derived, whose solution gave the drop size and the surfactant adsorption at given values of C_S^{INI} and Φ. As shown in ref 20, eq 4 described very well the experimental data for d_{32} in the surfactant-poor region 1, whereas the more sophisticated model was useful in describing the protein adsorption in the surfactant-rich region 2. Because the current study is centered around the effect of emulsifier concentration on mean drop size, we use below the simpler version of the model, eq 4.

(24) The maximal value of $\sigma_{OW} = 28$ mN/m, corresponding to the bare soybean oil/water interface (no surfactant), is used to make this estimate.

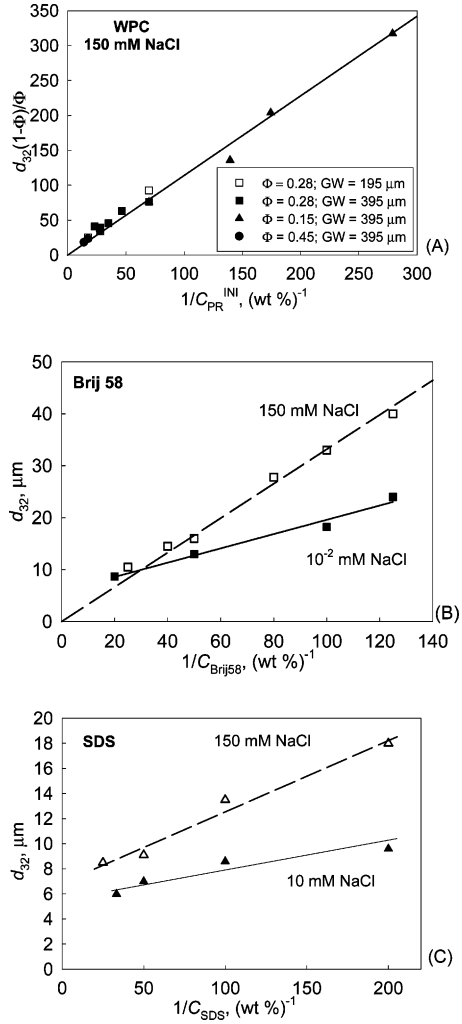

Figure 4. Mean diameter, d_{32}, as a function of the inverse initial emulsifier concentration for emulsions stabilized by (A) WPC, (B) Brij 58, and (C) SDS. The conditions during emulsification in parts B and C are the oil volume fraction, $\Phi = 0.28$, and gap width, GW = 395 μm.

From the slope of the best linear fit of the dependence $d_{32}(1 - \Phi)/\Phi$ versus $1/C_{PR}^{INI}$ (see eq 4 and Figure 4A), we determined $\Gamma^* = 1.9$ mg/m^2 for WPC solutions. The latter value is very close to the value for a dense protein monolayer, $\Gamma_M \approx 2$ mg/m^2, which was determined from the respective protein adsorption isotherm.[20] This result means that virtually a complete coverage of the drop surface by adsorbed protein, $\theta^* = \Gamma^*/\Gamma_M \approx 0.95$, is needed for preventing the drop re-coalescence, during emulsification, for WPC-stabilized emulsions. It was found in ref 20 that the values of Γ^* and θ^* did not depend on the oil volume fraction, Φ, and on the density of power dissipation, ϵ, which was an indication that Γ^* and θ^* could be considered as characteristics of the used emulsifier.

For the present study, we applied the same approach to determine the threshold surfactant adsorption, Γ^*, required for obtaining emulsions from Brij 58 + 150 mM NaCl solutions. From the best linear fit of d_{32} versus $1/C_{INI}$, we obtained $\Gamma^* = 1.4$ mg/m^2 for this system (see the dashed line in Figure 4B). This adsorption corresponds to an area per molecule $A^* = 1.33$ nm^2, which is about 2 times larger than the values reported in the literature for dense adsorption layers of Brij 58 at the air/water interface,[25,26] $A_M = 1/\Gamma_M \approx 0.65$ nm^2. We should note, however, that the adsorption at the soybean oil/water interface can be rather different from that at the air/water interface. As an example, Todorova et al.[27] found that the area per molecule in a saturated adsorption layer of the nonionic surfactant tridecyl-poly(ethylene oxide)-10 was about 2 times larger for the soybean oil/water interface, as compared to the air/water interface, $A_M = 1.13$ and 0.54 nm^2, respectively. Because the emulsions obtained in our experiments were very stable upon prolonged shelf storage (see section 3.5), we assume that a complete adsorption layer was formed during emulsification, which stabilizes the droplets by steric repulsion. In other words, $\Gamma_M \approx \Gamma^* = 1.4$ mg/m^2 and $\theta^* \approx 1$ are assumed for this system. We tried to determine Γ_M from interfacial tension isotherms, but this turned out to be a nontrivial task because of the very low critical micelle concentration, cmc $\approx 10^{-5}$ M ≈ 0.001 wt %, and the partial solubility of Brij 58 in the oil phase. Because the adsorption of a nonionic surfactant such as Brij 58 is not expected to depend strongly on NaCl concentration (except at very high electrolyte concentrations, where the salting out effect could become important), we assume the same value, $\Gamma_M \approx 1.4$ mg/m^2, for the system Brij 58 + 10^{-2} mM NaCl.

Our attempts to use eq 4 for estimating the threshold emulsifier adsorption, Γ^*, in the presence of Brij 58 at low electrolyte concentration (10^{-2} mM NaCl) and SDS (10 or 150 mM NaCl) were unsuccessful: The dependence of d_{32} on $1/C_{INI}$ exhibited a significant intercept, in contrast to the prediction of eq 4; see Figure 4B,C. This means that the simple phenomenological model is not applicable to these systems, and no specific values of Γ^* and θ^* can be defined as characteristics of the used emulsifier. To reveal the interrelation between surfactant concentration and adsorption in these systems, on one side, and mean drop size, on the other side, we analyze in the following the role of drop−drop interactions during emulsification.

3.3.2. Hydrodynamic Conditions in the Emulsification Chamber and in the Pipes of the Emulsification Equipment. The drop−drop coalescence could occur in various parts of the equipment: in the processing element and in the pipes (see Figure 1A). By estimating the respective Reynolds numbers, one can show that the flow is turbulent both in the processing element and in the pipes. The Reynolds number, $Re = HU\rho_C/\eta_C$, can be estimated from the linear velocity of the fluid, U, and the characteristic dimension, H. For the processing element, H is the width of the narrow slit, GW ≈ 395 μm, whereas outside the processing element H is to be associated with the pipe diameter, $2R_P \approx 1.6$ cm. From the known volumetric flow rate $Q \approx 130$ cm^3/s and the cross-sectional areas of the slit and of the pipes ($S = 0.086$ cm^2 and $S_P = 2.01$ cm^2, respectively), we calculated $U = Q/S = 15.1$ m/s and $Re \approx 6000$ in the processing element and $U = 0.65$ m/s and $Re \approx 10\,400$ in the pipes. As seen from these estimates, $Re \gg 1$ for both compartments of the equipment, which means turbulent flow.

There is a large difference between the hydrodynamic conditions in the processing element and those in the pipes, because the density of power dissipation in the pipes is much smaller. As explained in section 3.2, the density of power dissipation in the processing element is $\epsilon \approx 2.5 \times$

(25) Horozov, T.; Joos, P. Dynamic surface tension of surfactant solutions studied by peaktensiometry. *J. Colloid Interface Sci.* **1995**, *173*, 334.

(26) Petrov, P.; Joos, P. Linear compression of an adsorbed monolayer of a surfactant solution. *J. Colloid Interface Sci.* **1996**, *181*, 530.

(27) Todorova, D. T.; Marinova, K. G.; Gurkov, T. D.; Ivanov, I. B. Manuscript in preparation.

10^8 J/(m^3·s). The density of power dissipation in the pipes, $\epsilon_P = \Delta P_P Q/V_P$, can be estimated if the pressure drop along the pipes, ΔP_P, is known (V_P is the pipe internal volume). To estimate ΔP_P, we used the so-called "friction law", which connects the Reynolds number with the friction coefficient, χ, of the pipes in the turbulent regime[28]

$$\frac{1}{\sqrt{\chi}} = 0.88 \ln(Re\sqrt{\chi}) - 0.85 \quad (5)$$

By definition, the friction coefficient is related to the pressure difference and the average flow velocity, as follows:[28]

$$\chi = \frac{4R_P \Delta P}{\rho_C U^2 L_P} \quad (6)$$

where $L_P \approx 1$ m is the length of the pipes and $U = Q/S_P \approx 0.65$ m/s is the average flow velocity. Introducing $Re = 10\,400$ into eq 5, we estimate $\chi \approx 0.030$. Then, we find from eq 6 that $\Delta P_P \approx 400$ Pa, which corresponds to an average power density in the pipes $\epsilon_P \approx 300$ J/(s·m^3). Note that this value is 6 orders of magnitude smaller than the value of ϵ in the processing element. Introducing $\epsilon_P \approx 300$ J/(s·m^3) into eq 3, we obtain that the size of the smallest eddies in the pipes is $\lambda_{0P} \approx 43$ μm, which is larger than the drop size in all of the studied systems during emulsification (cf. with the results shown in Figure 2).

The above estimates show that, in the pipes, the drops are smaller than the turbulent eddies, $d < \lambda_{0P}$, which implies that the main hydrodynamic forces, exerted on the drops by the flow, are of *viscous* origin, while the pressure fluctuations related to *inertial* forces are of secondary importance.[1,6,22,23] In contrast, while traveling along the processing element, the drops are subjected mainly to inertial turbulent forces, because $d > \lambda_0$. These different flow regimes (viscous and inertial) lead to rather different drag forces on the drops in the different compartments of the equipment. That is why in the following we analyze separately the forces and the probability for drop−drop coalescence in the processing element and in the pipes.

We should note that, while we were able to measure the drop size distribution at the outlet of the pipes, we have no direct information about the mean drop size at the exit of the processing element. Nevertheless, as shown below, the analysis of the hydrodynamic forces and of drop−drop interactions (electrostatic and van der Waals) allows us to explain the measured mean drop size at the equipment outlet and to assess how intensive the coalescence was in the two different equipment compartments.

3.3.3. Evaluation of Emulsion Stability in the Processing Element. (A) Comparison of the Various Time Scales in the Processing Element. The simplest possible way to check whether the drop breakage and drop−drop coalescence are possible in a certain hydrodynamic flow is to estimate the characteristic times of the various "elementary" processes, which occur during emulsification.[1,6,23]

The average residence time of the emulsion droplets in the processing element, t_R, can be estimated from the ratio V_{DISS}/Q. From the characteristic values of the used element, $V_{DISS} \approx 1.7 \times 10^{-7}$ m^3 and $Q = 1.3 \times 10^{-4}$ m^3/s, we estimate $t_R \approx 1$ ms.

The process of drop deformation and breakage is characterized by the so-called "deformation time", t_{DEF}.

Table 1. Estimated Characteristic Times for Drops with Diameter d = 5, 10, and 20 μm[a]

characteristic time	d = 5 μm	d = 10 μm	d = 20 μm
residence time, t_R	1 ms	1 ms	1 ms
drop deformation time, t_{DEF}	9 μs	5 μs	3 μs
lifetime of an eddy with size d, t_{EDDY}	5 μs	7 μs	12 μs
time between two drop−drop encounters, t_{ENC}	1 μs	2 μs	3 μs
collision time, t_C	5 μs	7 μs	12 μs
adsorption time, t_A			
C = 0.01 wt %	100 μs	50 μs	25 μs
C = 1 wt %	1 μs	0.5 μs	0.25 μs

[a] See section 3.3.3A for the respective definitions and discussion.

According to Levich[23] and Walstra and Smulders,[1,6] t_{DEF} for viscous drops can be estimated from the expression

$$t_{DEF} \approx \frac{\eta_D}{5\rho_C^{1/3}\epsilon^{2/3}} \frac{1}{d^{2/3}} \quad (7)$$

where η_D is the dynamic viscosity of the drop (oil) phase and $\rho_C = 10^3$ kg/m^3 is the mass density of the continuous phase. Assuming $\epsilon = 2.5 \times 10^8$ J·m^{-3}·s^{-1} and $\eta_D = 50$ mPa·s, one estimates $t_{DEF} \approx 9$ μs for drops with diameter $d = 5$ μm, 5 μs for $d = 10$ μm, and 3 μs for $d = 20$ μm (see Table 1). Note that t_{DEF} is 2−3 orders of magnitude shorter than the residence time, which means that the drops have enough time for deformation and breakage while travelling along the processing element.

Another requirement for drop breakage is that t_{DEF} should be comparable to or shorter than the lifetime of the turbulent eddies of size $\lambda \sim d$ (the latter are expected to be most efficient in causing the drop breakage).[5,23] The meaning of this requirement is that the eddies, which create the pressure gradients in the oil−water mixture, should live sufficiently long, so that the oil drops have enough time to deform and break. According to the theory of turbulence, the average lifetime of such eddies is[6,28]

$$t_{EDDY} \approx \frac{\rho_C^{1/3}}{\epsilon^{1/3}} d^{2/3} \quad (8)$$

The estimates with $\epsilon = 2.5 \times 10^8$ J·m^{-3}·s^{-1} show that $t_{EDDY} \approx 5$ μs for $d = 5$ μm, 7 μs for $d = 10$ μm, and 12 μs for $d = 20$ μm. The comparison of t_{EDDY} with t_{DEF} shows that these characteristic times are similar in magnitude, which means that the eddies live sufficiently long to cause drop breakage, if d is above about 5 μm. In addition, one can show that the kinetic energy of the eddies, $E_{KIN} \sim \rho_C \langle u^2 \rangle d^3 \sim \rho_C^{1/3} d^{11/3} \epsilon^{2/3}$ (where $\langle u^2 \rangle \approx \epsilon^{2/3} \rho_C^{-2/3} d^{2/3}$ is the mean square velocity of a turbulent eddy with size d), is comparable to the surface energy of the drops, $E_S \sim \sigma_{OW} d^2$. The numerical estimates show that the ratio $E_{KIN}/E_S \approx (\rho_C^{1/3} \epsilon^{2/3} d^{5/3})/\sigma_{OW}$ is around 0.5, 2, and 6 for drops with diameters d = 5, 10 and 20 μm, respectively ($\sigma_{OW} = 10$ mN/m was used in these estimates).

In conclusion, all estimates predict that the turbulent flow is able to break rather efficiently drops with diameters larger than about 5 μm in the processing element of our equipment. A more detailed approach to the process of drop breakage, which leads to a similar conclusion, can be found in refs 5 and 29−33.

(28) Landau, L. D.; Lifshitz, E. M. In *Theoretical Physics*: *VI. Hydrodynamics*; Nauka: Moscow, 1988; Chapter 4 (in Russian).

(29) Calabrese, R. V.; Chang, T. P. K.; Dang, P. T. Drop breakage in turbulent stirred-tank contractors. Part I: Effect of dispersed-phase viscosity. *AIChE J.* **1986**, *32*, 657.

(30) Wang, C. Y.; Calabrese, R. V. Drop breakage in turbulent stirred-tank contractors. Part II: Relative influence of viscosity and interfacial tension. *AIChE J.* **1986**, *32*, 667.

In relation to drop−drop coalescence, one can estimate the average time between two consecutive encounters of a given drop with other drops, t_{ENC}, from the Kolmogorov's theory of turbulence, by using the following equation:[6]

$$t_{ENC} \approx \frac{\rho_C^{1/3}}{15\Phi\epsilon^{1/3}} d^{2/3} \quad (9)$$

Assuming $\Phi = 0.28$, one finds $t_{ENC} \approx 1\ \mu$s for $d = 5\ \mu$m, $t_{ENC} \approx 2\ \mu$s for $d = 10\ \mu$m, and $t_{ENC} \approx 3\ \mu$s for $d = 20\ \mu$m. The comparison of t_R and t_{ENC} shows that a given drop experiences a large number of encounters with other drops, $\sim 10^3$, during its passage through the processing element.

The probability for drop−drop coalescence in these encounters depends on the ratio of the so-called "collision time", t_C (which characterizes the mean duration of one collision) and the drainage time, t_{DR}, which characterizes how rapid the thinning of the film between two colliding drops is.[5] The collision time, t_C, can be estimated by the expression[5,6,33]

$$t_C \approx t_{EDDY} \approx \frac{\rho^{1/3}}{\epsilon^{1/3}} d^{2/3} \quad (10)$$

which gives $t_C \approx 5\ \mu$s for $d = 5\ \mu$m, 7 μs for $d = 10\ \mu$m, and 12 μs for $d = 20\ \mu$m.

The rate of film thinning and the respective drainage time, t_{DR}, strongly depend on the presence of surfactants on film surfaces.[34] An estimate of the characteristic adsorption time in the turbulent regime, t_A, can be made by the expression[6,23]

$$t_A \approx \frac{10\Gamma\eta_C^{1/2}}{C_S d\epsilon^{1/2}} \quad (11)$$

which accounts for the convective transport of surfactant toward the drop surface. C_S is the emulsifier concentration in the continuous phase. From the literature, we know that the monolayer adsorption is $\Gamma_M \approx 2.0$ mg/m^2 for WPC[20] and 1.4 mg/m^2 for Brij 58 and SDS.[8] Introducing typical values, $d \approx 5\ \mu$m and $\Gamma \approx 2$ mg/m^2 into eq 11, one obtains $t_A \approx 10^{-6}/C_S$ as an estimate, where C_S is expressed in wt %. This estimate predicts that the time scale of adsorption, t_A, depends strongly on emulsifier concentration.

The comparison of t_A, on one side, and the characteristic times of drop deformation and contact, t_{DEF} and t_C, shows that the adsorption could be faster or slower depending on surfactant concentration. At low surfactant concentration, about 0.01 wt %, the adsorption is expected to be slower than the processes of drop deformation and collision ($t_A \gg t_{DEF}$ and $t_A \gg t_C$, see Table 1). Hence, the drop−drop encounters probably occur between droplets, whose surfaces are covered with less dense, nonequilibrium adsorption layers. In contrast, at high emulsifier concentrations, about 1 wt %, the adsorption process is expected to occur in the time scale of 1 μs (i.e., $t_A \ll t_{DEF}$ and $t_A \ll t_C$), which suggests that the drop surfaces are covered by adsorption layers, whose density is close to the equilibrium one.

Note that the transition between the surfactant-rich and the surfactant-poor regimes occurred at similar surfactant concentrations in all studied systems, $C_S^{INI} \sim 0.1$ wt %. As the estimates show, t_A becomes comparable to t_{DEF} and t_C at approximately the same surfactant concentration for all systems, ~0.1 wt %. Therefore, the coalescence in the surfactant-poor regime probably occurs between droplets whose surfaces are covered with dilute nonequilibrium adsorption layers.

Let us emphasize that the adsorption time is much shorter than the residence times, $t_A \ll t_R$, for all studied systems in our experiments. Furthermore, we used multiple passes (around 100) of the emulsion through the processing element, before taking samples for measuring d_{32}. These multiple passes ensure steady-state drop size distribution and provide additional time for completion of the adsorption process inside the homogenizer (including the pipes). That is why we do not consider explicitly the kinetics of emulsifier adsorption in our analysis.

At the present moment, there is no adequate theoretical approach to estimate reliably the drainage time, t_{DR}, for drops in turbulent flow. This problem is discussed at the end of the following subsection B.

(B) Magnitude of Turbulent Hydrodynamic Force and Formation of Thin Films between Colliding Drops. The probability for drop−drop coalescence depends strongly on the hydrodynamic force, which pushes the drops against each other, and on the surface forces (van der Waals, electrostatic, etc.), which act between the drops, when the latter are separated by a small gap of thickness h. The pushing hydrodynamic force can be estimated as being a fraction of the mean turbulent drag force, F_T, which is given by the expression[9]

$$F_T \sim d^2\rho_C\langle u^2\rangle \sim d^{8/3}\rho_C^{1/3}\epsilon^{2/3} \quad (12)$$

Assuming $d = 5\ \mu$m, $\rho_C = 10^3$ kg/m^3, and $\epsilon = 2.5 \times 10^8$ J/(m^3·s), one estimates $F_T \approx 3 \times 10^{-8}$ N.

On the basis of theoretical arguments, one can show that a thin emulsion film, with more or less planar surfaces, is expected to form between two colliding drops in the processing element. Indeed, when two drops approach each other under the action of an external force, F_{EX}, a planar film must form when the dynamic pressure in the gap between the drops becomes comparable to the drop's capillary pressure.[35] According to the theory, the planar film is formed at the so-called "inversion thickness", which is estimated from the equation[35]

$$h_{INV} = \frac{F_{EX}}{2\pi\sigma_{OW}} \quad (13)$$

The radius of the formed film can be estimated by equalizing F_{EX} to the hydrodynamic force, created by the viscous dissipation in the film. In its own turn, the viscous dissipation force is equal to the product of the hydrodynamic pressure in the film (which is equal to the drop

(31) Calabrese, R. V.; Wang, C. Y.; Bryner, N. P. Drop breakage in turbulent stirred-tank contractors. Part III: Correlations for mean size and drop size distribution. *AIChE J.* **1986**, *32*, 677.

(32) Narsimhan, G.; Ramkrishna, D.; Gupta, J. P. Analysis of drop size distributions in lean liquid−liquid dispersions. *AIChE J.* **1980**, *26*, 991.

(33) Tsouris, C.; Tavlarides, L. L. Breakage and coalescence models for drops in turbulent dispersions. *AIChE J.* **1994**, *40*, 395.

(34) Ivanov, I. B. Effect of surface mobility on the dynamic behavior of thin liquid films. *Pure Appl. Chem.* **1980**, *52*, 1241.

(35) Ivanov, I. B.; Dimitrov, D. S. Thin film drainage. In *Thin Liquid Films: Fundamentals and Applications*; Ivanov, I. B., Ed.; Marcel Dekker: New York, 1988; Chapter 7.

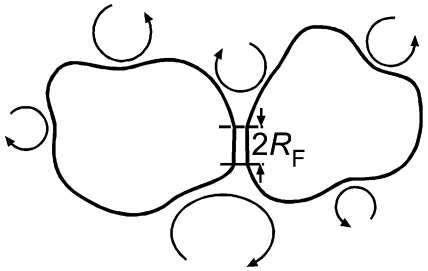

Figure 5. Schematic presentation of drops with diameter much larger than the diameter, d_K, calculated by eq 2.

capillary pressure) multiplied by the film area. Hence, the equation for the film radius reads[34,35]

$$R_F^2 = \frac{F_{EX}}{\pi P_{CAP}} \quad (14)$$

Assuming that the external force, pushing the drops against each other, is the turbulent drag force, $F_{EX} \approx F_T$, and that $P_{CAP} \approx 4\sigma_{OW}/d$, one derives

$$h_{INV} \approx \frac{d^{8/3}\rho_C^{1/3}\epsilon^{2/3}}{2\pi\sigma_{OW}} \quad (15)$$

$$R_F^2 \approx \frac{d^{11/3}\rho_C^{1/3}\epsilon^{2/3}}{4\pi\sigma_{OW}} \quad (16)$$

From eqs 15 and 16, one can estimate $h_{INV} \sim 0.5\,\mu$m and $R_F \sim 1\,\mu$m for drops with $d = 5\,\mu$m in the processing element [$\sigma_{OW} = 10$ mN/m, $\epsilon = 2.5 \times 10^8$ J/(m^3·s)]. For drops with $d = 10\,\mu$m, one obtains $h_{INV} \sim 3\,\mu$m and $R_F \sim 4\,\mu$m. Therefore, one can conclude from these estimates that planar films are expected to form between the drops in the processing element as a result of the large magnitude of the turbulent force, F_T.

One should note, however, that eq 16 predicts unrealistically large values, $R_F > d/2$, for the bigger drops in the studied systems, $d \geq 20\,\mu$m. This discrepancy could be anticipated, because the pressure fluctuations in the turbulent flow field are larger than the capillary pressure of the bigger drops with diameter $d > d_K$ (d_K is the drop diameter calculated by eq 2). As a result, these large drops are deformed by the turbulent flow and the approximation of their shape by spheres (for single drops) or truncated spheres (for colliding drops) is not justified. As a result, the diameter of the films, formed between such drops, could be smaller than the prediction of eq 16; see Figure 5 as an illustration.

From the viewpoint of drop−drop coalescence kinetics, it would be of considerable interest to analyze the rate of thinning and to estimate the respective drainage time t_{DR} of the films formed between colliding drops. However, t_{DR} depends very strongly on the film radius, R_F, and on the critical film thickness, h_{CR}, at which the film rupture occurs.[35] In addition, the drainage time depends strongly on the presence of surfactants, adsorbed on the film surfaces (so-called "Marangoni effect").[1,6,34,35] Because there are no reliable theoretical expressions for R_F, h_{CR}, and the Marangoni effect, we refrain from considering the dynamics of planar film thinning and rupture in the current article. Furthermore, the analysis of the kinetic aspects of drop breakup and drop−drop coalescence requires a detailed account of the interaction between the drops and the turbulent flow field. We tried to apply some of the existing kinetic theories[5,33] to describe our experimental data, but we found that either the quantitative description is impossible or we need to introduce a significant number of parameters with unclear physical meaning and unjustified values. That is why we are currently performing further experimental and theoretical work to clarify and quantify the kinetic aspects of the emulsification process; the respective results will be described in a subsequent study.

In the present study, we analyze the film stability from the viewpoint of the colloidal surface forces, which stabilize or destabilize the film at a certain thickness (i.e., the kinetic aspect is not considered). As explained in the following, we were able to explain almost all of our results for the steady-state mean drop size, by considering only the surface forces. The only exception is the system Brij 58 + 10^{-2} mM NaCl. As explained in section 3.3.5, the results for the latter system can be explained qualitatively by the combined action of a Marangoni effect in the processing element and electrostatic repulsion in the pipes of the equipment.

(C) Electrostatic Barrier in the Planar Films Intervening between Two Colliding Drops in the Processing Element. When a planar film is formed between two colliding drops, its stability can be analyzed by comparing the capillary pressure, P_{CAP} (which is the driving force for film thinning), with the disjoining pressure, $\Pi(h)$, which may stabilize the film, if sufficiently strong repulsion between the film surfaces occurs.[36] If P_{CAP} is smaller than the height of the barrier in the disjoining pressure isotherm, Π_{MAX}, there is an equilibrium film thickness, h_{EQ}, at which $P_{CAP} = \Pi(h_{EQ})$ and the net driving force for film thinning, $P_{CAP} - \Pi$, is equal to 0. In such a case, one may expect that the drops will rebound after their encounter, without coalescence. In contrast, if $P_{CAP} > \Pi_{MAX}$, there is no equilibrium film thickness and the film stability is determined by the ratio of the contact time, t_C, and the drainage time, t_{DR}. In our systems, $P_{CAP} \approx \sigma_{OW}/d$ is on order of 10^3−10^4 Pa.

To evaluate theoretically the height of the electrostatic barrier, stabilizing the emulsion films, we consider the electrostatic and van der Waals contributions into the disjoining pressure isotherm:

$$\Pi = 64 n_0 k_B T \left[\tanh\left(\frac{e\Psi_s}{4k_B T}\right)\right]^2 \exp(-\kappa h) - \frac{A_H}{6\pi h^3} \quad (17)$$

where n_0 is the electrolyte number concentration, $k_B T$ is the thermal energy, κ is the inverse Debye screening length, Ψ_S is the electrical surface potential of the drops, e is the elementary charge, A_H is the Hamaker constant, and h is the film thickness.

Because Ψ_S is a function of the surfactant adsorption, we calculated the disjoining pressure isotherms, $\Pi(h)$, for different values of Ψ_S, which were varied in the range between the surface potential of the bare oil/water interface (without adsorbed surfactant, $\theta \approx 0$) and the potential corresponding to maximal surfactant adsorption ($\theta \approx 1$). The electrostatic potential of the oil/water interface was determined by measuring the electrophoretic mobility of soybean oil drops and calculating their ζ potential. For simplicity, we assume in the theoretical estimates that the measured ζ potential is equal to the surface potential of the drops, Ψ_S. The electrophoretic measurements were made at the various NaCl concentrations studied, in the absence and in the presence of surfactant. The instrument

(36) Kralchevsky, P. A.; Danov, K. D.; Denkov, N. D. Chemical physics of colloid systems and interfaces. In *Handbook of Surface and Colloid Chemistry*; Birdi, K. S., Ed.; CRC Press LLS: Boca Raton, 1997; Chapter 11.

Table 2. Calculated Barriers to Drop−Drop Coalescence in the Processing Element, Π_{MAX}/P_{CAP}, and in the Pipes, F_{MAX}/F_P[a]

system	θ	Ψ_S, mV	Π_{MAX}/P_{CAP}	F_{MAX}/F_P
SDS + 10 mM NaCl	0	−40	10	10^4
	1	−120	10^2	10^5
SDS + 150 mM NaCl	0	0	0	0
	0.22	−21	≈1	<1
	0.23	−22	>1	≈1
	1	−50	10^2	10^4
WPC + 150 mM NaCl	0	0	0	0
	1	−10	0	0
Brij 58 + 150 mM NaCl	0	0	0	0
	1	0	0	0
Brij 58 + 10^{-2} mM NaCl	0	−80	0.1	10^3
	1	−15	10^{-3}	10^2

[a] The values $P_{CAP} = 5000$ Pa and $F_P = 10^{-13}$ N are used in these estimates. $\theta = \Gamma/\Gamma_M$ is the adsorption coverage of the drop surface, and Ψ_S is the respective electrical surface potential (see sections 3.3.3 and 3.3.4 for explanations).

Malvern 2c (Malvern Instruments, U.K.) was used, and the procedures described in ref 37 were followed.

The experiments showed that the ζ potentials of the bare soybean oil/water interface (no surfactant, $\theta \approx 0$) are $\zeta \approx -80$ mV for 10^{-2} mM, ≈ -40 mV for 10 mM, and ≈ 0 for 150 mM NaCl, respectively. These results are very close to the data presented in ref 37 for several other nonpolar oils, at the same NaCl concentrations and pH ≈ 6. As explained in refs 37 and 38, this surface potential is created by adsorbed hydroxyl ions on the bare oil−water interface. The ζ potentials of oil droplets, covered with adsorption monolayers of the studied emulsifiers ($\theta \approx 1$), are presented in Table 2.

For the following analysis of emulsion stability, it is convenient to define a threshold surface potential, Ψ_T, at which the height of the electrostatic barrier, Π_{MAX}, becomes equal to P_{CAP}; see Figure 6A. Because the surface potential of the drops, Ψ_S, depends on surfactant adsorption, Ψ_T corresponds to a certain threshold surface coverage, θ_T, at which $\Pi_{MAX} = P_{CAP}$.

In Table 2, we show the calculated disjoining pressure barriers, Π_{MAX}, normalized by the capillary pressure, $P_{CAP} \approx 5 \times 10^3$ Pa, for the studied emulsifiers, at several values of Ψ_S. The respective surface coverage, θ, is also shown. The values of the other parameters, used to calculate the theoretical curves $\Pi(h)$ by eq 17 and to find Π_{MAX}, are $A_H = 10^{-20}$ J and $\kappa^{-1} = 3.04$ or 0.785 nm for 10 or 150 mM NaCl, respectively.

As seen from Table 2, Ψ_S varies between −40 mV (bare oil−water interface, $\theta = 0$) and −120 mV (saturated adsorption monolayer) for the system SDS + 10 mM NaCl. The calculations showed that $\Pi_{MAX} > P_{CAP}$ in the entire range of possible values of Ψ_S for this system (see Table 2). This means that the drops, stabilized by SDS + 10 mM NaCl, should not coalesce in the processing element, even at very small surface coverage by surfactant, as a result of the high electrostatic barrier in this system.

For the emulsion stabilized by SDS in the presence of 150 mM NaCl, the calculated threshold surface potential

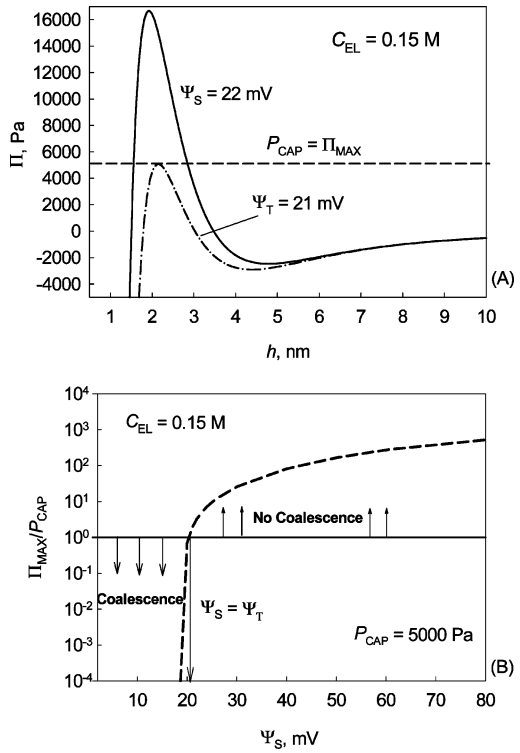

Figure 6. (A) Calculated electrostatic disjoining pressure, Π, as a function of the film thickness, h, at $C_{EL} = 0.15$ M; (B) calculated dependence of Π_{MAX}/P_{CAP} on Ψ_S at $C_{EL} = 0.15$ M ($P_{CAP} = 5000$ Pa). The other parameters used in the calculations are $A_H = 10^{-20}$ J and $T = 300$ K.

is $\Psi_T = -21$ mV; see Figure 6A. One can relate Ψ_T to the SDS adsorption, Γ, by using the Gouy equation[36]

$$\sigma_S = -\alpha e\Gamma = (8\epsilon_r\epsilon_0 k_B T n_0)^{1/2} \sinh\left(\frac{e\Psi_S}{2k_B T}\right) \quad (18)$$

where σ_S is the surface charge density, e is the elementary charge, $\epsilon_r \approx 80$ is the relative dielectric permittivity of the aqueous phase, and ϵ_0 is the dielectric permittivity in vacuo. We assume $\alpha \approx 0.2$ as the degree of dissociation of the SDS molecules in the adsorption layer.[39,40] Substituting $\Psi_S = \Psi_T = -21$ mV into eq 18, we calculated that that the respective threshold surfactant adsorption is $\Gamma_T \approx 6.0 \times 10^{17}$ molecules/m^2, which corresponds to a surface coverage $\theta_T \approx 0.22$ (according to ref 8, $\Gamma_\infty \approx 2.7 \times 10^{18}$ molecules/m^2). This estimate suggests that drops with surface coverage $\theta < \theta_T$ could coalesce in the processing element by overcoming the electrostatic barrier, whereas drops with $\theta > \theta_T$ should not coalesce, because $\Pi_{MAX} > P_{CAP}$ for them.

For WPC-stabilized emulsions, the measured surface potential of the bare oil−water interface $\Psi_S(\theta = 0) \approx 0$ and the calculated threshold potential, $\Psi_T \approx -21$ mV, are similar to those in the system SDS + 150 mM NaCl, because the ionic strength is the same. On the other hand, we measured the ζ potential of emulsion drops, stabilized by 0.5 wt % WPC (i.e., at $\theta \approx 1$) to be only −10 mV, which is about two times lower than the estimated value of Ψ_T needed for electrostatic stabilization of the films. There-

(37) Marinova, K. G.; Alargova, R. G.; Denkov, N. D.; Velev, O. D.; Petsev, D. N.; Ivanov, I. B.; Borwankar, R. Charging of Oil−Water Interfaces due to Spontaneous Adsorption of Hydroxyl Ions. *Langmuir* **1996**, *12*, 2045.

(38) Karraker, K. A.; Radke, C. J. Disjoining pressures, zeta potentials and surface tensions of aqueous nonionic surfactant/electrolyte solutions: theory and comparison to experiment. *Adv. Colloid Interface Sci.* **2002**, *96*, 231.

(39) Kralchevsky, P. A.; Danov, K. D.; Broze, G.; Mehreteab, A. Thermodynamics of Ionic Surfactant Adsorption with Account for the Counterion Binding: Effects of Salts of Various Valency. *Langmuir* **1999**, *15*, 2351.

(40) Kalinin, V. V.; Radke, C. J. An ion-binding model for ionic surfactant adsorption at aqueous-fluid interfaces. *Colloids Surf.* **1996**, *114*, 337.

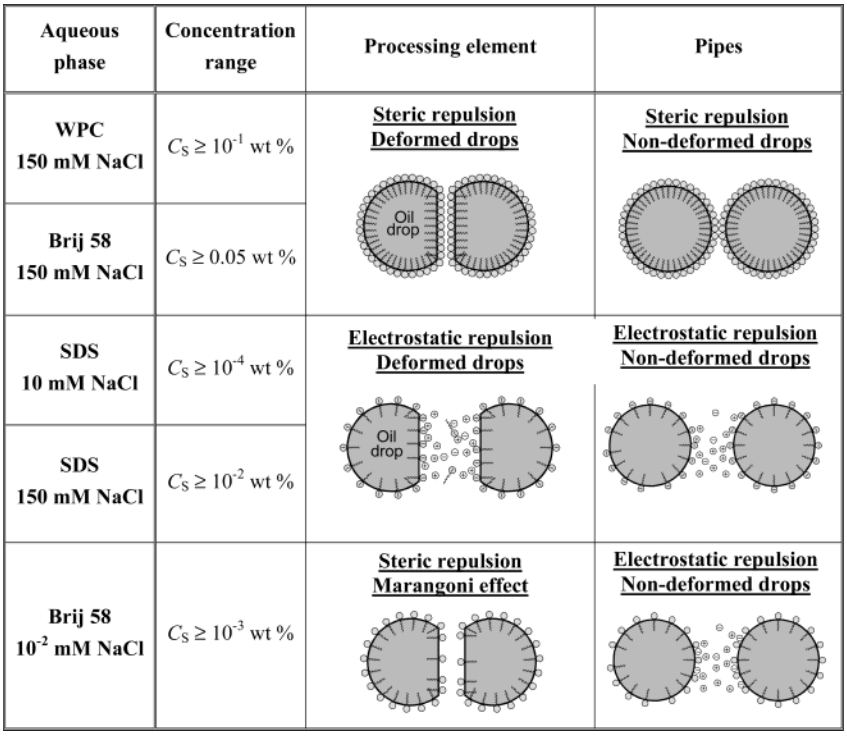

Figure 7. Schematic presentation of the main factors controlling drop stability against coalescence, during emulsification, in the studied systems.

Table 3. Calculated Theoretical Threshold Surface Coverage, θ_T, for Suppressing Drop−Drop Coalescence in the Different Compartments of the Used Homogenizer[a] along with the Experimentally Determined Surface Coverage at the outlet of the Emulsification Equipment, θ_{OUT}, and after Emulsion Shelf Storage for 24 h, θ_{ST}[b]

			theoretical degree of coverage, θ_T, needed for drop stabilization		experimental surface coverage, calculated from surfactant mass balance	
N	system	Γ_M, mg/m^2	processing element	pipes	outlet of emulsification equipment	after 24 h of shelf storage
1	WPC + 150 mM NaCl	2.0	$\theta_T \approx 1$; steric repuslion	$\theta_T \approx 1$; steric repulsion	$\theta_{OUT} \approx 1$	$\theta_{ST} \approx 1$
2	Brij 58 + 150 mM NaCl	1.4	$\theta_T \approx 1$; steric repuslion	$\theta_T \approx 1$; steric repulsion	$\theta_{OUT} \approx 1$	$\theta_{ST} \approx 1$
3	SDS + 10 mM NaCl	1.4	$\theta_T \approx 0$; electrostatic repulsion	$\theta_T \approx 0$; electrostatic repulsion	$\theta_{OUT} < 0.05$	$\theta_{ST} \approx 0.4$
4	SDS + 150 mM NaCl	1.4	$\theta_T \approx 0.22$; electrostatic repulsion	$\theta_T \approx 0.23$; electrostatic repulsion	$\theta_{OUT} \approx 0.3$	$\theta_{ST} \approx 1$
5	Brij 58 + 10^{-2} mM NaCl	1.4	$\theta_T \approx 1$; steric repuslion	$\theta_T \approx 0$; electrostatic repulsion	$\theta_{OUT} \approx 0.8$	$\theta_{ST} \approx 1$

[a] Processing elements and pipes. [b] Γ_M is the emulsifier adsorption in a dense monolayer.

fore, the electrostatic repulsion is not sufficiently strong to prevent the drop−drop coalescence in WPC-stabilized emulsions, because $\Pi_{MAX} < P_{CAP}$ at any value of θ between 0 and 1 (see Table 2). Thus, we can conclude that the oil drops in this system would coalesce by overcoming the electrostatic barrier unless the steric repulsion, created by the adsorbed protein molecules, becomes sufficiently strong to stabilize the films. Because the adsorption layer of WPC molecules in region 1 consists mainly of compact (globular) protein molecules,[20] one can expect that the steric repulsion would become significant only when the film surfaces are armored by a relatively dense adsorption layer (i.e., at $\theta \approx 1$).

For drops stabilized by Brij 58, we found that the calculated values of Π_{MAX} are much smaller in magnitude than P_{CAP} for any value of the surface coverage, θ, at both electrolyte concentrations studied, 10^{-2} and 150 mM NaCl; see Table 2. This means that the electrostatic barrier is too low to prevent the drop−drop coalescence in the processing element for Brij-stabilized emulsions. Hence, intensive coalescence is expected to occur in these systems until the adsorption layer becomes sufficiently dense to create a significant steric repulsion between the film surfaces. However, as discussed by Walstra,[1,6,8] the coalescence can be efficiently suppressed by the Marangoni effect (which decelerates the drainage of the planar films) for low molecular mass surfactants; this point is discussed in section 3.4.

Let us summarize here the results from the comparison of the electrostatic barrier, Π_{MAX}, and the capillary pressure, P_{CAP}, for all studied systems; see Figure 7 and Table 3. Coalescence by overcoming the electrostatic barrier is possible for Brij 58 with and without NaCl; WPC with 150 mM NaCl; and SDS in the presence of 150 mM NaCl (in the latter case only at $\theta < \theta_T \approx 0.22$). Stabilized by the electrostatic barrier are the SDS emulsions at 10 mM NaCl and those in the presence of 150 mM NaCl at $\theta > \theta_T \approx 0.22$.

3.3.4. Evaluation of Emulsion Stability in the Pipes of the Equipment. (A) Hydrodynamic Force and Drop Shape in the Pipes. The size of the smallest eddies in the pipes is larger than the size of the biggest emulsion drops in the

studied systems (43 vs 40 μm). As a result, the hydrodynamic drag force, acting on the drops in the pipes, is a *viscous* turbulent force, which is very different from the *inertial* turbulent force in the processing element. The hydrodynamic viscous force, exerted on dispersed drops by turbulent eddies of larger size, $d < \lambda_0$, was estimated by Levich[23]

$$F_P \approx \frac{\pi}{2\sqrt{3}} d^3 \rho_C^{-1/2} \Delta\rho \epsilon_P^{3/4} \eta_C^{-1/4} \tag{19}$$

where $\epsilon_P \sim 300$ J/(m^3·s) is the density of energy dissipation in the pipes and $\Delta\rho = 80$ kg/m^3 is the difference between the mass densities of the oil and water phases. From eq 19, one estimates $F_P \approx 10^{-13}$ N for drops with diameter $d \approx 5$ μm. Note that this force is 5 orders of magnitude smaller, as compared to the hydrodynamic drag force in the processing element, F_T (viz., eq 12). It is worthwhile to note that an alternative expression for the estimate of F_P was proposed by Chesters:[41]

$$F_P \approx 6\pi\eta_C (d/2)^2 \dot{\gamma}_T \approx \frac{3}{2}\pi d^2 (\eta_C \epsilon_P)^{1/2} \tag{20}$$

where $\dot{\gamma}_T = (\epsilon_P/\eta_C)^{1/2} \approx 547$ s^{-1} is the characteristic rate of strain of the viscous flow inside the smallest turbulent eddies. Equation 20 predicts different numerical values for the hydrodynamic force (e.g., $F_P \approx 6 \times 10^{-11}$ N for drops with $d \approx 5$ μm) and different dependences on drop size. Nevertheless, our numerical estimates showed that both expressions for F_P lead to the same conclusions in our analysis. In the further consideration, we use the values provided by eq 19, because its derivation is somewhat more elaborate in comparison with the simpler scaling arguments used to derive eq 20.

Introducing $F_P \approx 10^{-13}$ N into eq 13, one estimates that the inversion thickness for film formation in the pipes should be $h_{INV} < 0.1$ nm. This inversion thickness is much smaller than the expected value of the critical thickness for film rupture, h_{CR} (for unstable films), or than the equilibrium film thickness, h_{EQ} (for stable films). Moreover, by using eq 14 with $F_{EX} \approx F_P$, one can show that the film radius (if a planar film is formed at all) should be 4 orders of magnitude smaller than the drop diameter, $R_F/d \approx 10^{-4}$. Let us mention also that the capillary number, $Ca = \tau_{VISC}/P_{CAP} = \eta_C \dot{\gamma}_T d/(2\sigma_{OW}) \approx 8 \times 10^{-5}$, is much smaller than unity, which means that the drops are not deformed by the viscous flow of the continuous medium. All these estimates show that the drops in the pipes can be adequately modeled as nondeformed spheres and their stability could be analyzed by comparing the electrostatic barrier for *spheres* with the hydrodynamic force, calculated by eqs 19 or 20.

(B) Electrostatic Barrier for Spherical Drops. To account for the electrostatic barrier between two colliding spherical drops, we consider the interaction force, F_{SP}, as a superposition of electrostatic and van der Waals contributions (e.g., ref 36)

$$F_{SP} = \frac{64\pi}{\kappa} n_0 k_B T \left[\tanh\left(\frac{e\Psi_S}{4k_B T}\right)\right]^2 \exp(-\kappa h) R - \frac{A_H R}{12h^2} \tag{21}$$

where h is the distance between the foreheads of the drops and R is the drop radius.

(41) Chesters, A. K. The modelling of coalescence processes in fluid-liquid dispersions: A review of current understanding. *Chem. Eng. Res. Des.* **1991**, *69*, 259.

A comparison of the maximal repulsive force between two spherical drops, F_{MAX} (which is the height of the electrostatic barrier in this case), and the hydrodynamic force in the pipes, F_P, is presented in Table 2. This comparison suggests that the coalescence stability of the drops in the pipes should be as follows:

For emulsions stabilized by SDS + 10 mM NaCl and by Brij 58 + 10^{-2} mM NaCl, the electrostatic barrier is higher than the hydrodynamic force, $F_{MAX} > F_P$, at arbitrary surface coverage of the drops. This means that coalescence in the pipes, by overcoming the electrostatic barrier, is improbable.

For the system SDS + 150 mM NaCl, the threshold surface potential, at which F_{MAX} becomes larger than F_P, is $\Psi_T \approx -22$ mV. Coincidentally, this value of Ψ_T is almost the same as the value estimated above for planar emulsion films in the processing element. By using eq 18, one estimates that −22 mV corresponds to a threshold surface coverage $\theta_T \approx 0.23$.

For emulsions stabilized by WPC + 150 mM NaCl and Brij 58 + 150 mM NaCl, the electrostatic repulsion is unable to create a barrier. Therefore, the coalescence in these systems is expected to proceed until a sufficiently strong steric repulsion between the drops appears.

3.4. Comparison of the Theoretical Predictions with the Experimental Results for the Mean Drop Size during Emulsification (Region 1). In this section, we compare the theoretical predictions about the surface coverage of the emulsion drops in the surfactant-poor region 1 (see sections 3.3.3C and 3.3.4B) with the experimental results.

First, we explain how the experimental data for d_{32} were processed to estimate the surface coverage of the drops at the outlet of the emulsification equipment, θ_{OUT}. Note that θ_{OUT} depends on the initial surfactant concentration for the electrostatically stabilized systems Brij 58 + 10^{-2} mM NaCl and SDS (for the other two systems θ_{OUT} is practically constant, cf. Figure 4 and eq 4). The comparison of the theoretical estimates for the threshold surface coverage, θ_T, with the experimental values θ_{OUT}, is made for $d_{32} \approx 13$ μm. This value of d_{32} was chosen because, as explained at the end of section 3.2, the drop size in all emulsions with $d_{32} > 13$ μm is certainly affected by drop−drop coalescence. Therefore, $d_{32} \approx 13$ μm denotes the boundary between the emulsions, which are strongly affected by coalescence, and those that are only slightly affected.

To calculate θ_{OUT} from the measured values of d_{32} for WPC and Brij-containing emulsions, we used the relation

$$\theta_{OUT} = \frac{\Gamma_{OUT}}{\Gamma_M} = \frac{1-\Phi}{6\Phi} \frac{C_S^{INI}}{\Gamma_M} d_{32} \tag{22}$$

which is a direct corollary of eq 4. As explained in section 3.3.1, eq 4 implies that virtually all emulsifier is adsorbed on the drop surfaces at the end of emulsification. The latter assumption was verified in ref 20 for WPC-stabilized emulsions. For Brij 58, this assumption is also justified. Indeed, although its critical micelle concentration, cmc ≈ 0.001 wt %, is much lower than the initial concentration of the used surfactant solutions, $C_S^{INI} \geq 0.01$ wt %, the surfactant concentration in the aqueous phase, in the surfactant-poor region 1, should be close to or smaller than cmc $\ll C_S^{INI}$ at the end of the emulsification process. Otherwise, the micelles would act as a reservoir, able to supply surfactant for further adsorption and reduction of drop size, which is not the case in the actual experiments. Hence, in the mass balance, one can neglect the amount of Brij 58 in the aqueous phase, which leads to eq 22.

However, eq 22 is not applicable to SDS-stabilized emulsions, because the cmc of this surfactant is comparable to C_S^{INI} in region 1. Therefore, one should explicitly account for the partitioning of SDS between the drop surfaces and the aqueous phase. That is why we used the adsorption isotherm, $\Gamma(C_{SDS})$, to make the surfactant mass balance for this system.[20] $\Gamma(C_{SDS})$ at the soybean oil/water interface was determined in ref 27 by following the procedure of Rehfeld;[42] the experimental interfacial tension isotherm $\sigma_{OW}(C_{SDS})$ was interpolated by a series of logarithmic functions, which were afterward introduced into the Gibbs adsorption isotherm:

$$\sigma = A_0 + A_1 \ln(C_S) + A_2 \ln^2(C_S) + ... \quad (23)$$

$$\Gamma = -\frac{1}{kT}\frac{d\sigma}{d\ln(C_S)} = -\frac{1}{kT}[A_1 + 2A_2 \ln(C_S)] \quad (24)$$

The following values were obtained[27] from the best fit of the experimental data: $A_0 = -217.9$, $A_1 = -29.01$, *and* $A_2 = -0.8684$ for 10 mM NaCl and $A_0 = -171.9$, $A_1 = -18.97$, and $A_2 = -0.4509$ for 150 mM NaCl, where C_S is expressed in mol/cm^3 and σ_{OW} in mN/m. Following the approach from section 3.6 in ref 20, we combined the adsorption isotherm with the surfactant mass balance to obtain the following transcendental equation for the determination of C_S^{SER} in the stirred, SDS-stabilized emulsions

$$\frac{(1-\Phi)(C_S^{INI} - C_S^{SER})d_{32}}{6\Phi} = -\frac{A_1 + 2A_2 \ln(C_S^{SER})}{RT} \quad (25)$$

As an example, for the system SDS + 150 mM NaCl, the initial surfactant concentration, at which $d_{32} = 13\ \mu$m, is $C_S^{INI} = 0.01$ wt %, which corresponds to 3.46×10^{-7} mol/cm^3. Introducing the latter value and $d_{32} = 13\ \mu$m into eq 25, we obtain for $C_S^{SER} = 8.5 \times 10^{-8}$ mol/cm^3, which corresponds to $\Gamma_{OUT} = 0.4$ mg/m^2 (from eq 24) and $\theta_{OUT} = 0.3$, respectively.

All experimental results for θ_{OUT}, determined as explained previously, are compared in Table 3 with the theoretical predictions for the threshold values, θ_T (see also Figure 7):

(1) WPC + 150 mM NaCl and (2) Brij 58 + 150 mM NaCl. The theoretical consideration predicts that there is no significant electrostatic barrier in these systems. Therefore, the coalescence should proceed until a sufficiently strong steric repulsion appears at $\theta_T \approx 1$. In agreement, we found experimentally $\theta_{OUT} \approx 1$ at all studied surfactant concentrations. The physical explanation of this result is that, in these systems, the drops coalesce during emulsification until θ becomes ≈ 1. Once a sufficiently dense adsorption layer is formed, it ensures a strong steric repulsion, which stabilizes the drops against further coalescence. This should be the typical case when no significant electrostatic repulsion occurs between the drops.

(3) SDS + 10 mM NaCl. The theoretical estimates predict that no coalescence is expected to occur in this system, even at $\theta_T \approx 0$, as a result of the electrostatic repulsion between the drops, which is strong enough to prevent drop−drop coalescence, even at a vanishing SDS adsorption. In agreement, we found that the surface coverage, determined from the experimental data for d_{32}, is very low: $\theta_{OUT} < 0.05$ (see Table 3). The absence of significant drop−drop coalescence in this system is supported also by the fact that d_{32} is described very well by the Kolmogorov−Hinze theory of emulsification at all studied SDS concentrations (section 3.2 and Figure 3B).

(4) SDS + 150 mM NaCl. The predictions for this system are that the emulsion drops would coalesce in both the processing element and the pipes, if the surface electric potential is lower than −22 mV, which corresponds to $\theta_T \approx 0.23$. Experimentally, we found that the degree of coverage at the outlet is around 0.3 (slightly higher than the theoretical estimate) for the emulsions with d_{32} comparable to the prediction of Kolmogorov−Hinze theory. This experimental result means that the emulsion drops with $\theta \geq 0.3$ are stabilized against coalescence during emulsification by electrostatic repulsion.

(5) Brij 58 + 10^{-2} mM NaCl. The theoretical prediction is that no significant electrostatic barrier exists for this system, in the processing element. Therefore, from the viewpoint of the electrostatic interactions, the drops should coalesce in the processing element until a sufficiently strong steric repulsion appears. For the pipes, the theoretical prediction is that the electrostatic repulsion precludes the drop−drop coalescence; see Table 3. Experimentally, at the outlet of the equipment, we obtained a surface coverage, $\theta_{OUT} \approx 0.8 < 1$ (see Table 3), which is slightly lower than what is needed for steric stabilization. The most probable explanation for the experimentally observed θ_{OUT} is that the drop−drop coalescence was decelerated by the Marangoni effect in the processing element. That is, the adsorbed Brij molecules decelerated the drainage of the liquid films, formed between colliding drops, so that $t_{DR} > t_C$ and the drops had no time to accomplish the coalescence process. As a result, the drops entered into the pipes with incomplete surface coverage, where they were stabilized by electrostatic repulsion (section 3.3.4B and Table 2).

We should mention that the Marangoni effect could be of some importance for the other systems as well, but it was apparently overwhelmed in our experiments by other, more important effects and phenomena—by the electrostatic repulsion for SDS and by the steric repulsion for Brij 58 + 150 mM NaCl.

In conclusion, the surface coverage found experimentally at the outlet of the equipment, θ_{OUT}, is explained by the following factors (see also Table 3): SDS + 10 mM NaCl, $\theta_{OUT} \approx 0.05$ due to electrostatic repulsion; SDS + 150 mM NaCl, $\theta_{OUT} \approx 0.3$ due to electrostatic repulsion; WPC + 150 mM NaCl and Brij 58 + 150 mM NaCl, $\theta_{OUT} \approx 1$ due to steric repulsion; and Brij 58 + 10^{-2} mM NaCl, $\theta_{OUT} = 0.8$ due to Marangoni effect in the processing element and to electrostatic repulsion in the pipes.

3.5. Estimate of the Threshold Surface Coverage Needed To Obtain Emulsions with Long-Term Stability. The values of θ_{OUT} just discussed are related to the emulsification process and must be distinguished from the surface coverage, θ_{ST}, needed to ensure long-term emulsion stability. That is why we made additional experiments to determine θ_{ST} and to compare it to θ_{OUT}.

To determine θ_{ST}, we stored the emulsions for 24 h. After this period of shelf storage, some of the emulsions (depending on the emulsifier type and concentration) remained stable, while in the others, a bulk oil layer was released on top of the emulsion cream. The mean drop diameter in the stable emulsions was measured after 24 h to be the same as the one measured immediately after emulsification. For this reason, the release of bulk oil was used as an indicator for the lack of long-term emulsion stability. For SDS-stabilized emulsions, we estimated C_S^{SER} and θ_{ST} by using eqs 24 and 25. For the other systems,

(42) Rehfeld, S. J. Adsorption of sodium dodecyl sulfate at various hydrocarbon−water interfaces. *J. Phys. Chem.* **1967**, *71*, 738.

no such detailed calculations were needed (see the following explanations).

The main results from these experiments can be summarized as follows (see Table 3):

(1) WPC + 150 mM NaCl, and (2) Brij 58 + 150 mM NaCl. No separation of free oil was observed during the shelf-storage period at all studied concentrations (down to 0.01 wt %). This means that the spontaneous coalescence process had been accomplished during emulsification and the surface coverage does not change upon shelf storage, that is $\theta_{ST} = \theta_{OUT} \approx 1$.

(3) SDS + 10 mM NaCl. We found that virtually all oil separated at $C_{SDS}^{INI} = 10^{-3}$ wt %, whereas no oil was found to separate at $C_S^{INI} = 0.01$ wt %. From the mean drop size in the latter system, $d_{32} \approx 8.6$ μm, and making a mass balance (eqs 24 and 25), we estimated that $\theta \approx 0.4$ in this stable emulsion. Therefore, a relatively strong electrostatic repulsion leads to an efficient stabilization of these emulsions, even at low surface coverage, $\theta_{ST} < 0.4$.

(4) SDS + 150 mM NaCl. At $C_S^{INI} < 0.02$ wt %, almost all of the oil used for emulsion preparation spontaneously separated during the first 5 min after the end of the emulsification process. The initial surfactant concentration at which the emulsions were stable was found to be 0.2 wt %. The latter concentration is well above cmc $\approx$ 0.03 wt % ($\approx$1 mM at 150 mM NaCl), and, hence, a dense adsorption layer, with $\theta \approx 1$, is expected to form in equilibrium. These results show that $\theta_{ST} \approx 1 > \theta_{OUT} \approx 0.3$ for this system.

(5) Brij 58 + 10^{-2} mM NaCl. The emulsions with Brij 58 + 10^{-2} mM NaCl were also unstable upon shelf storage, when the surfactant concentration was below about 0.1 wt %. A fraction of the emulsified oil separated after 24 h of shelf storage. However, we were unable to estimate the area of the oil−water interface in these unstable emulsions and to determine θ_{ST} because no clear boundary between the separated oil and the remaining stable o/w emulsion could be seen (the separated oil phase contained tiny water droplets).

In conclusion, the threshold surface coverage for obtaining stable emulsions was estimated as follows: $\theta_{ST} \approx 1$ for WPC, Brij 58, and SDS (all with 150 mM NaCl) and $\theta_{ST} \approx 0.4$ for SDS + 10 mM NaCl.

4. Conclusions

A systematic experimental study is performed to reveal the effects of emulsifier type and concentration and of NaCl concentration on the mean drop size, d_{32}, during emulsification in turbulent flow. An anionic surfactant (SDS), a nonionic surfactant (Brij 58), and a protein emulsifier (WPC) are studied, and the results are analyzed by considering the drop−drop interactions during emulsification. The main results can be summarized as follows:

(1) In the surfactant-rich regime, $C_S^{INI} > 0.1$ wt %, d_{32} does not depend on surfactant concentration and is determined by the interfacial tension (which is a characteristic of the used surfactant) and by the density of power dissipation, ϵ, in the emulsification chamber. The measured values of d_{32} are described very well by the Kolmogorov−Hinze theory of emulsification for all studied systems; see eq 2 and Figure 3. All emulsions obtained in the surfactant-rich regime were stable for days upon shelf storage.

(2) In the surfactant-poor regime, $C_S^{INI} < 0.1$ wt %, d_{32} strongly depends on the initial surfactant concentration. From the linear dependence of d_{32} versus $1/C_S^{INI}$, we determined the threshold emulsifier adsorption for obtaining emulsions, Γ^*, in the systems stabilized by WPC + 150 mM NaCl or Brij 58 + 150 mM NaCl; see eq 4 and Figure 4. In a previous study,[20] we showed that Γ^* does not depend on the oil volume fraction and ϵ, which means that Γ^* can be considered as a characteristic of the used emulsifier. The analysis performed in the present study shows that this is the typical case when no significant electrostatic repulsion occurs between the drops. In such systems, the drops coalesce during emulsification until Γ becomes equal to Γ^*. Once a sufficiently dense adsorption layer is formed, it ensures a strong steric repulsion, which stabilizes the drops against further coalescence. During shelf storage, these emulsions remain stable, which indicates that Γ^* coincides with the adsorption ensuring a long-term emulsion stability, Γ_{ST}.

(3) If a significant electrostatic barrier is present in the surfactant-poor regime (SDS + 10 or 150 mM NaCl and Brij 58 + 0.01 mM NaCl), the emulsifier adsorption strongly depends on the emulsification conditions. Hence, no threshold emulsifier adsorption, Γ^*, could be defined for these systems. Moreover, the obtained emulsions were rather unstable upon shelf storage, which means that the surfactant adsorption at the outlet of the emulsification equipment, Γ_{OUT}, was considerably lower than Γ_{ST}.

(4) The transition between the surfactant-rich and the surfactant-poor regimes occurred at similar surfactant concentrations in all studied systems, $C_S^{INI} \sim 0.1$ wt % [for the used oil volume fraction $\Phi = 0.28$ and $\epsilon = 2.5 \times 10^8$ J/(m^3·s)]. The analysis of the various characteristic times, related to the emulsification process in our equipment, showed that the adsorption time, t_A, becomes comparable to the drop deformation time, t_{DEF}, and to the collision time, t_C, at $C_S \approx 0.1$ wt %. Therefore, the coalescence in the surfactant-poor regime occurs between droplets whose surfaces are covered with under-saturated, nonequilibrium adsorption layers.

The performed theoretical estimates of the electrostatic barrier to drop−drop coalescence allowed us to explain the measured drop size, d_{32}, and the surfactant adsorption at the outlet of the emulsification equipment, Γ_{OUT}, in the studied systems (section 3.4). Some interesting conclusions can be drawn from the theoretical consideration:

(5) The drop−drop coalescence could occur both in the processing element and in the pipes of the emulsification equipment. In contrast, the drop breakage occurs exclusively in the processing element because of the much higher density of power dissipation there.

(6) In the processing element, the colliding drops are deformed (as a result of the high value of ϵ) and thin emulsion films are formed between them, whereas the drops can be considered as spherical in the pipes of the equipment.

(7) The stability of the emulsion films, formed between colliding drops in the processing element, is determined by the ratio of the height of the electrostatic barrier in the disjoining pressure isotherm, Π_{MAX}, and the drop capillary pressure, P_{CAP}. In contrast, the stability of the spherical drops in the pipes is determined by the relative magnitudes of the repulsive barrier (in terms of interdroplet surface force, F_{MAX}) and the hydrodynamic drag force, which pushes the drops against each other, F_P. In general, these different criteria for realization of the drop−drop coalescence may correspond to different threshold surfactant adsorptions for the pipes and for the processing element, respectively.

The above conclusions support and complement the results from previous articles (e.g., refs 1, 2, 6, 8, 19, and 20) and provide deeper insight into the role of surfactant type and concentration in the emulsification process. We continue our study with additional experimental and

theoretical efforts, aimed to quantify the role of surfactants and electrolytes in terms of the rates of drop breakage and drop−drop coalescence, and to describe the initial, nonstationary stage of drop size reduction during emulsification.

Acknowledgment. The authors are indebted to Professor Ivan B. Ivanov (Sofia University) for the numerous discussions throughout the study; his valuable help is gratefully acknowledged. We would like to thank BASF AG for the support of this study and for the permission to publish its results. The authors of ref 27 are acknowledged for the permission to use their results prior to publication. The contributions of Dr. V. Valchev (for the homogenizer preparation) and of Dr. D. Sidzhakova (for performing part of the emulsification experiments) are also gratefully acknowledged.

LA049335A